

## Columnar defects induced by high energy heavy ions in HTSC. Their effect on irreversibility line and pinning properties.

V. Hardy, J. Provost, D. Groult, Ch. Simon, M. Hervieu, B. Raveau

Laboratoire CRISMAT,  
URA 1318 (CNRS)  
ISMRA /Université de Caen  
6 Boulevard du Maréchal Juin  
14050 CAEN - Cedex, France

### Abstract

The defects induced by high energy heavy ions have been studied by high resolution electron microscopy. Columnar amorphous defects of 7 nm in diameter have thus been characterized in the case of 6 GeV-Pb ion irradiation of Y-123, Bi-2212 and Tl-2212 superconductors. Because of their diameter close to the coherence length  $\xi$  and their shape similar to the vortex core they have been demonstrated as the best pinning centers that can be introduced in HTSC. Drastic changes of the magnetic hysteresis and critical current density are thus reported. Volume pinning force modifications and strong shifts of the irreversibility line have been studied as a function of the temperature and the columnar defect density i.e. the ion dose. The magnetic field dependence of the critical current density has been discussed on the basis of a competition between pinning and vortex repulsion.

### 1. Introduction

Magnetic properties studies of high  $T_c$  materials have shown the existence of the irreversibility line (IL)(1) at the boundary of a broad reversible region in their B-T. (magnetic field-temperature) phase diagram. In the reversible region the flux line lattice (FLL) can move under the action of the Lorentz force and the critical current density  $j_c$  vanishes. The origin of this line is still not well understood and raises the question of FLL behavior against applied magnetic field, temperature and pinning. In low  $T_c$  materials pinning is mainly governed by crystal lattice defects. The situation is not so clear in HTSC in which the layered structure results in highly anisotropic properties and can play a role in FL pinning. Nevertheless the ability of extended defects to act as pinning centers should be studied.

The production of defects by irradiation with various particles like neutrons(2,3) protons(4) and heavy ions(5-8) is a powerful tool to study the pinning in HTSC. From this view point, heavy ion irradiation connected with high resolution electron microscopy (HREM) investigations can be very useful. Indeed, it offers the possibility to put clearly in relation some modifications of the IL with a homogeneous and very well characterized set of defects (nature, shape, dimensions, density and spatial distribution).

To explain IL a lot of models have been proposed which invoke very different phenomena as thermally activated depinning(9,10) or phase transitions in the vortex lattice (1,11-13). One of the key points in this debate is the precise role of the defects. At the beginning, the diversity of compounds and projectiles used did not

allow to extract clear conclusions : neutron irradiation of Bi-2212 crystals led to a strong shift of the IL (14), but, on the opposite, proton irradiation of Y-123 crystals had no effect despite a great enhancement of  $j_c$  (15). More recently, heavy ion irradiations have considerably enlightened the situation. Strong shifts of the IL towards high fields and temperatures were systematically observed with all the compounds studied (6,8,16-18). Induced defects are very different from the preexisting ones and have a much greater pinning ability. This is likely the reason why these columnar defects have led to displacements of the IL contrary to defects too similar to the preexisting ones as, for instance, those created by protons in Y-123 (15). As a result, heavy ion irradiation experiments have greatly contributed to demonstrate the connection between the defects and the IL. Nevertheless, the exact relations between the structure of defects and the location of the IL are not yet well known.

Moreover, the values of  $B_{max}$  corresponding to the field of the maximum of the volume pinning force  $F_p$  ( $F_p = j_c B$ ) depends also on the induced defect density. The present work has been more specially devoted to strong changes of pinning forces and irreversibility line of Bi-2212 crystals irradiated by 6 GeV-Pb ions.

### 2. Experimental

#### 2.1. Sample preparation and HREM

Single crystals of Bi-2212 type HTSC were prepared as previously described(8). The HREM investigations were carried out using a TOPCON 002B electron microscope equipped with an objective lens whose spherical aberration constant is  $C_s = 0.4$  mm. The single

crystals were smoothly crushed in alcohol and deposited on a holey carbon coated grid. Microcrystals suitable for HREM observations were also obtained by cryofracture in liquid nitrogen and then dispersed in n-butanol or alcohol and collected on copper grids.

### 2.2. Irradiation procedure

Irradiations were carried out at 300 K. The flux of the ion beam was limited to  $2 \times 10^8$  ions  $\text{cm}^{-2}\text{s}^{-1}$  in order to avoid warming effects during irradiation. The Bi-2212 single crystals were irradiated along their smallest direction i.e. the c-axis, within an angle resolution of about  $5^\circ$  from it. In all the experiments the ion range was much larger than the crystal thickness and the defects induced by heavy ions can be mainly ascribed to electronic energy loss effects.

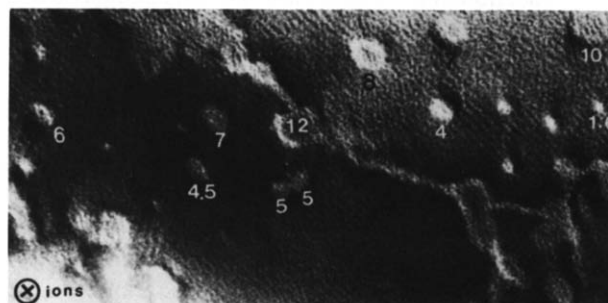
### 2.3. Magnetic measurements

All magnetic measurements prior to and following heavy ion irradiation were carried out with the DC magnetic field aligned parallel to the c direction. The field

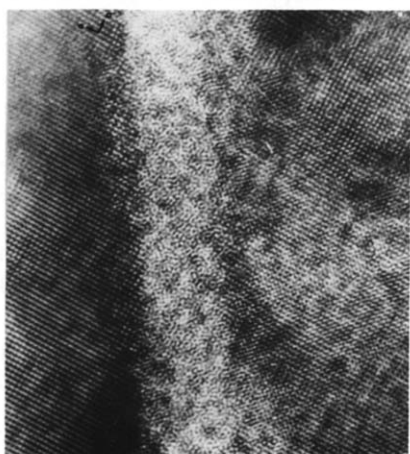
was roughly oriented along the c-axis ( $\pm 5^\circ$ ) but tests of reproducibility have shown that this uncertainty is not relevant on experimental results reported here. The magnetization hysteresis loops, the field cooled (FC) and zero field cooled (ZFC) magnetizations were recorded with a Quantum Design 5.5 T SQUID magnetometer. Hysteresis loops were recorded up to 5 Tesla and down to zero field. The sample was previously cooled down to the working temperature in zero field. The FC and ZFC data were collected after 60 s of waiting time and 3 scans of 2 cm length as in hysteresis loop measurements. Precautions were taken in a temperature range of about 10-15 K around the irreversibility temperature which was recorded by steps of 1 K. The irreversibility lines reported in this paper were achieved by the determination of the merging point of FC and ZFC curves. In practice, the criterion that we used to define the "reversible" behaviour corresponds to a current density  $j < 10$  A/cm<sup>2</sup>. The magnetic critical current density  $j_c$  and the volume pinning force  $F_p$  have been inferred from hysteresis loops  $M(B)$  at fixed temperature.



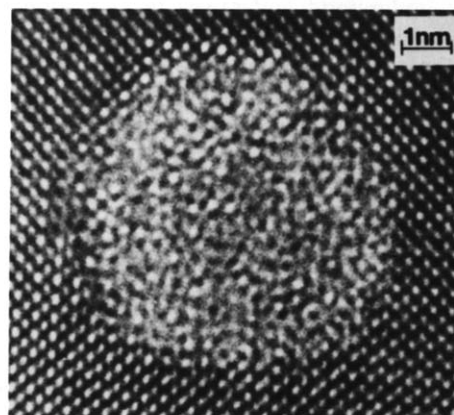
(a)



(b)



(c)



(d)

Figure 1 (a) Discontinuous latent track of 5.8 GeV-Xe ions in Tl-2212 (side view)  
 (b) Top view of 5.8 GeV-Xe ions in Tl-2212 : the apparent size of the tracks range from 1.5 to 12 nm.  
 (c) High resolution image (a-b plane) of a 5.3 GeV-Pb ion latent track ( $\phi = 6.10^{11}$  cm<sup>-2</sup>) aligned parallel to the ion beam in Y-123 material.  
 (d) High resolution (a-b plane) top view (same irradiation conditions as in (c)).

### 3. Latent track formation induced by high energy heavy ions in HTSC materials.

Two nearly independent mechanisms are responsible for defect production in matter irradiated by swift heavy ions. The nuclear stopping power  $S_n = -(dE/dx)_n$  results from elastic collisions between the projectile ion and the target nuclei and the electronic stopping power  $S_e = -(dE/dx)_e$  which results from inelastic collisions with the target electrons. In all the experiments described here,  $S_e$  is more than three orders of magnitude higher than  $S_n$ :  $S_e/S_n > 10^3$ . We have shown for the first time (19) from 3.5 GeV-Xe irradiation of Y-123 ceramics that  $S_e$  plays a major role in the defect creation mechanism provided a threshold value of the energy deposited by electronic stopping is exceeded. This value has been estimated from in-situ resistance measurements close to 8 MeV/ $\mu\text{m}$  for Y-123 ceramics, single crystals and thin films. As  $S_e$  increases, the defect structure changes from discontinuous extended defects along the ion path to continuous amorphous cylindrical tracks (19,20) when  $S_e$  exceeds a new threshold value close to 20 MeV/ $\mu\text{m}$  in Y-123. Figure 1(a) shows a side view of discontinuous latent tracks of 5.8 GeV-Xe ions in Tl-2212 and figure 1(b) a top view of tracks induced by 5.8 GeV-Xe ions in Tl-2212. In this latter case the apparent size of the tracks varies from 1.5 to 12 nm which shows that the defect distribution in the target is not homogeneous.

Figures 1 (c) and 1 (d) show a continuous amorphous cylindrical track induced by a 5.3 GeV-Pb ion in Y-123 ( $S_e > 35$  MeV/ $\mu\text{m}$ ). Such amorphous defects have a nearly constant diameter (7 nm) across the sample. They are expected to act as very efficient pinning centers as their diameter is close to the coherence length  $\xi_{ab}$ .

### 4. Volume pinning force $F_p$

The origin of the temperature and magnetic field dependences of the volume pinning forces  $F_p$  in high  $T_c$  superconductor materials is at the present time the subject of intense activity since it controls the value of the critical current density  $j_c$  ( $F_p = j_c B$ ). The vortex lattice shear constant  $C_{66}$  and the pinning centers should play a fundamental role in the control of the pinning force (21), but this remains still obscure (22). In classical type II superconductors, there is a scaling law for the pinning force:

$$F_p(T, B) = F_p^{\max}(T) f(b) \quad (1)$$

where  $b = B/B_m$ , with  $B_m = B_{c2}$  being the upper critical field. The function  $f$  is not temperature dependent and presents a maximum (23). In high  $T_c$  superconductors, it has been shown that  $B_{c2}$  should be replaced by the irreversibility field  $B_m = B_{irr}$  where the critical current

vanishes (24). This indicates that the same mechanism controls both the irreversibility line and the pinning force near this maximum. The interpretation of the shape of the function  $f$  in Y-123 remains controversial since some authors mainly discussed the role of the lattice rigidity (25) while others neglected it completely and introduced mainly the thermally activated flux creep (24). The creation of a controlled number of defects with a controlled geometry can be a good test of these theories.

We report here data corresponding to magnetic fields above the field of complete penetration  $B^+$ . Since the samples are thin, the internal magnetic field is close to the applied field and is quite homogeneous even at low temperature ( $B^+ (6 \text{ K}) = 1000 \text{ G}$ ). To calculate  $j_c$  from the hysteresis loops, we have studied  $\Delta M$ , the difference between the two branches of the cycle. Before irradiation, it should be outlined that  $\Delta M$  presents the same temperature and magnetic field dependences for all the crystals which have been investigated. Nevertheless, there is a slight dispersion in the absolute values of  $\Delta M$  which could be related to the difference of dimensions between the samples. We have chosen the proportionality factors ( $j_c = \alpha \Delta M$ ) leading to the same value of  $j_c$  for all the samples before irradiation, and then, we have used these same factors to obtain  $j_c$  after irradiation. In this study, we were more interested by the field and temperature dependences of  $j_c$  or its relative variation due to irradiation than by its absolute values.

Four different Bi-2212 single crystals were irradiated at fluences of  $10^{10}$ ,  $5.10^{10}$ ,  $10^{11}$  and  $2.10^{11}$  Pb/cm<sup>2</sup>. They exhibited  $T_c$ 's near 85K and their dimensions were about  $(1 \times 1 \times 0.02) \text{ mm}^3$ . Before irradiation, the irreversibility lines of the 4 samples were identical. In the discussion, we will introduce the dose equivalent field  $B_{\phi t}$  which is defined as  $B_{\phi t} = n_{\phi t} \phi_0$ , where  $\phi_0$  is the elementary flux quantum and  $n_{\phi t}$  the track density. In such a notation, the fluences considered here above correspond to dose equivalent fields of 0.2, 1, 2 and 4 T. At  $B = B_{\phi t}$ , there is "one vortex per track".

In the considered range of fluence, the  $T_c$  is only slightly altered. For the highest fluence, the  $T_c$  decrease is less than 10 % and there is not yet any broadening of the transition.

Before irradiation, all the crystals that we used exhibit the same behavior of the volume pinning forces. In agreement with the published results on this material (26), we observe a scaling law according to formula (1) with a maximum at a given value of the magnetic field  $B_{\max}^0$ .  $F_p$  vanishes at a field  $B_{irr}^0$ , the ratio  $B_{\max}^0/B_{irr}^0$  being roughly constant and equal to about 1/4. In the following, the superscript <sup>0</sup> refers to the sample before irradiation.

After irradiation, a new maximum appears. On figure (2), we have shown  $F_p$  as a function of  $B$  at 15K before and after irradiation at  $B_{\phi t} = 0.2$  Tesla. Though  $j_c$  is decreasing over the whole range of magnetic field, there are two maxima in the pinning force after irradiation.

Such an observation of a two peak structure in  $F_p$  is quite new, though it was already reported in non irradiated Y-123 thin films and interpreted by considering two different types of pinning centers (27).

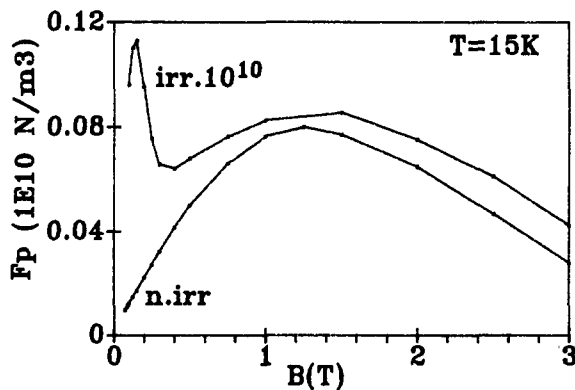


Figure 2 Pinning forces at 15K of a Bi-2212 crystal before irradiation (n.irr.) and after (irr.  $10^{10}$ ) at  $B_{\phi_t} = 0.2T$ .

Figure 2 demonstrates without any ambiguity that the new peak is related to the creation of the new columnar defects. Since the density and the nature of these new defects are known, it is possible to compare the density of vortices to the density of defects. As pointed out in figure 2, there is a good agreement between the position  $B_{max}$  of the maximum and the dose equivalent field  $B_{\phi_t} = 0.2$  Tesla. In the following,  $B_{max}$  will refer to the new peak observed in irradiated samples and  $B_{max}^0$  to the maximum which already exists in the non irradiated samples, since this maximum does not move significantly with dose.

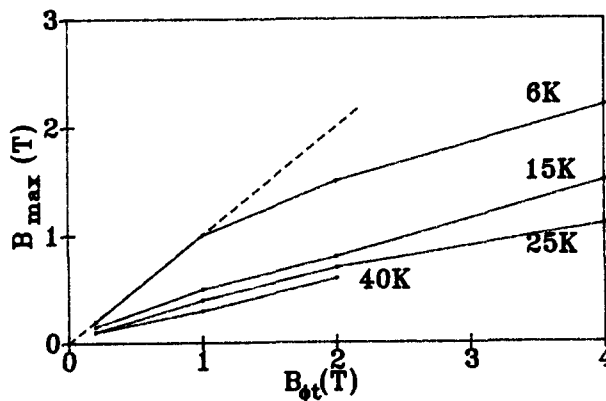


Figure 3 The  $B_{\phi_t}$  dependence of  $B_{max}$  for different temperatures. The dotted line corresponds to  $B_{max} = B_{\phi_t}$ .

In figure 3, we have reported the values of  $B_{max}$  corresponding to the field of the maximum of  $F_p$  as a function of  $B_{\phi_t}$  for different temperatures. At 6K, one observes that  $B_{max}$  is nearly equal to  $B_{\phi_t}$  for  $B_{\phi_t}$  smaller than 1 Tesla and then deviates for  $B_{\phi_t}$  larger than 2 Tesla. At temperature higher than 6K, the values of

$B_{max}$  are systematically smaller than  $B_{\phi_t}$  for the whole range of  $B_{\phi_t}$ . However, it remains proportional to  $B_{\phi_t}$  up to 2Tesla. This linear dependence of  $B_{max}$  is due to the particular geometrical configuration in which the vortex lattice is aligned parallel to the columnar defects. Such a geometry should explain the difference between Pb ion irradiation and proton irradiation which creates point defects and does not move  $B_{max}$  (28). Neutrons which create cascades of atomic displacements move  $B_{max}$  but without any correlation with the number of induced extended defects (29).

Note also that the value of the ratio  $B_{max} / B_{\phi_t}$  decreases as the fluence increases and as the temperature increases. This can be interpreted by the competition between the pinning energy and the repulsive energy between vortices. The ratio between the pinning energy to the repulsive energy is proportional to  $\ln(d/\lambda_{ab})$  where  $\lambda_{ab}$  is the London length and  $d$  the distance between vortices. As temperature increases,  $\lambda_{ab}$  increases and the depinning is larger. As the fluence increases, the average distance  $d$  between vortices decreases and the depinning also is larger. Such an effect was already observed in Pb-Bi superlattices where the pinning is due to the Bi layers. The equivalent of  $B_{\phi_t}$  is  $\Phi_0 / a^2$  ( $a$  is the periodicity of the superlattice) (30,31). Note also that the distribution of the tracks is not periodic which can increase the depinning. At high temperatures, the flux creep effect must be taken into account in the depinning process (22).

### 5. Irreversibility line

#### 5.1. The shift of the irreversibility line.

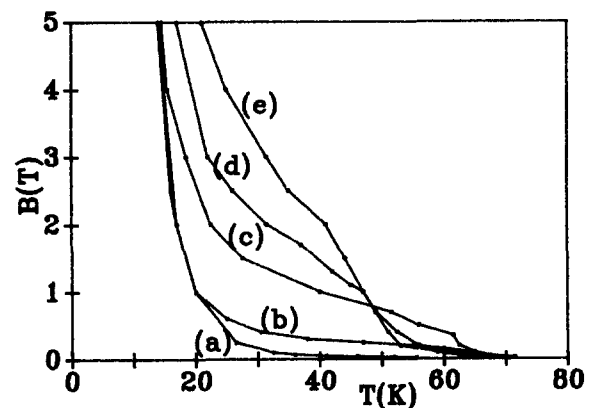


Figure 4 The c-axis irreversibility line of Bi-2212 single crystals before and after irradiation by different fluences of 6 GeV-Pb ions : (a) : 0 ; (b) :  $10^{10} \text{cm}^{-2}$ ; (c) :  $5 \cdot 10^{10} \text{cm}^{-2}$ ; (d) :  $10^{11} \text{cm}^{-2}$ ; (e) :  $2 \cdot 10^{11} \text{cm}^{-2}$ .

We have previously reported preliminary results on the strong shift of the IL of a Bi-2212 crystal irradiated by 6 GeV-Pb ions at a fluence of  $2 \cdot 10^{11} \text{Pb/cm}^2$  (8). We present here a detailed study of the relations between the

track density and the IL displacement. We have studied the same crystals and the same fluences as for the pinning force investigation.

Figure 4 presents the irreversibility lines of the Bi-2212 single crystals before irradiation and after the 4 different fluences of Pb ions. Firstly, it appears clearly that the introduction of efficient pinning centers like the tracks can lead to strong shifts of the IL towards higher fields and temperatures. This result has already been discussed (8) and it contributes to demonstrate that pinning has to be taken into account in models concerned with the origin of the IL. Moreover, we observe on figure 4 that the amplitude of the shift is strongly related to the density of defects and that the shape of the line is deeply modified. These effects were not so clear and systematic in the previous studies of irradiation effects on the IL. Concerning the shape modification, a very net change of regime at a field close to  $(B_{\phi t} / 2)$  appears on the "irradiated" lines (see, for instance, the knee at 5000 G on the line corresponding to  $5.10^{10}$  Pb/cm<sup>2</sup>). The same results that in figure 4 are reported in figure 5 in a semilog plot versus the reduced temperature  $t=T/T_c$ .

This representation allows to display clearly the whole field range and also to correct the slight reduction of  $T_c$  induced by the irradiation. It appears that at least 3 ranges of temperature have to be distinguished in order to describe the IL shift :

(1) in a large domain of intermediate temperatures (about between  $t \approx 0.3$  and  $t \approx 0.6$  for the studied range of fluence), the lines are strongly displaced towards the high fields. The amplitude of displacement increases with the track density.

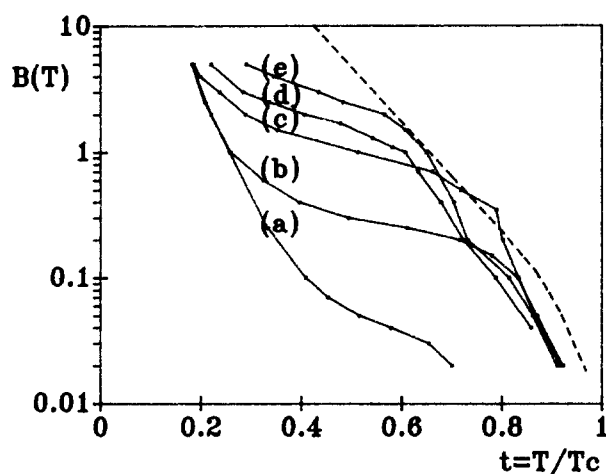


Figure 5 The same data as in figure (4) presented in a semilog plot versus the reduced temperature  $t = T/T_c$ : a):0; (b): $10^{10}$ cm<sup>-2</sup>; (c):  $5.10^{10}$ cm<sup>-2</sup>; (d):  $10^{11}$ cm<sup>-2</sup>; (e): $2.10^{11}$ cm<sup>-2</sup>.The dashed line is the 3D-2D transition proposed by H. Raffy et al.(32).

(2) at lower temperatures, the lines tend to join the one before irradiation. This behaviour is particularly clear for the lowest fluence (curve (b) in figures 4 and 5. The superposition begins at a field as low as the fluence is.

(3) at higher temperatures, all the lines corresponding to the different fluences tend to coincide far below  $T_c$ .

Let us now comment each of these 3 regimes.

### 5.2. The intermediate temperature range:

We observe that not only the displacement increases with the defect density but the irreversibility fields of each "irradiated line" are actually centered around the corresponding  $B_{\phi t}$  value. Let us now consider a simple relation :  $B_{irr}(T) \approx B_{\phi t}$  without dealing with the more complex dependence of the lines in this regime. The existence of such a strong relation between  $B_{irr}$  and  $B_{\phi t}$  originates from the very peculiar geometric aspect of the problem : indeed, in our case, the vortices and the defects form two sets of colinear tubes with nearly the same diameters ( $\xi_{ab}(0) \approx 40 \text{ \AA}$  (33)).

According to the above relation between  $B_{irr}(T)$  and  $B_{\phi t}$ , a dissipation occurs as soon as the vortex density becomes larger than the track one. So, in the simplest approach, we can consider that the origin of the IL within this temperature range comes from the necessity of an individual vortex pinning. The existence of this kind of matching between the vortices and the *random* tracks distribution tends to indicate that the shear modulus ( $C_{66}$ ) is quite weak at those temperatures. This qualitative  $B_{irr}(T) \approx B_{\phi t}$  relation is the major characteristic of the intermediate temperature range but it cannot be forgotten that, in fact,  $(B_{irr}/B_{\phi t})$  decreases as  $T$  or  $B_{\phi t}$  increases.

This can be interpreted by a competition between the pinning energy and the repulsive energy between vortices as stated above for the ratio  $B_{max}/B_{\phi t}$ .

### 5.3. The low temperature range:

This range corresponds to the part of the lines superimposed to the one before irradiation. This merging effect is very net and  $B_{irr}$  becomes rapidly much higher than  $B_{\phi t}$  (see curve (b) on figures 4 and 5. Consequently, one can think that the mechanism at the origin of the IL within this low-T range is strictly the same as before irradiation.

### 5.4. The high temperature range:

The transition between this regime and the regime of intermediate temperatures is well defined as shown in figure 6 for a fluence of  $10^{11}$  Pb/cm<sup>2</sup> by the appearance of a crossover between the two regimes. One observes that the IL within the high-T range can still be described by an exponential law. We observe that the track density has no more important role since all the irradiated lines are nearly superimposed in this high-T range. Therefore, it appears reasonable to relate the apparition of this regime to an intrinsic limit. With a compound as anisotropic as Bi-2212, the first phenomenon that can be

considered is the 3D-2D transition of the vortex lattice. Several studies have been carried out on this subject (34-39) and the problem is still not clearly resolved. However, it should be outlined here that there is a remarkable correlation between our results and the decoupling line proposed by H. Raffy et al (32). From magnetoresistive measurements on Bi-2212 thin films, those authors found evidence of a line in the (B,T) plane above which giant 2D fluctuations occur. We have checked that this line also exists in the Bi-2212 crystals that we used.

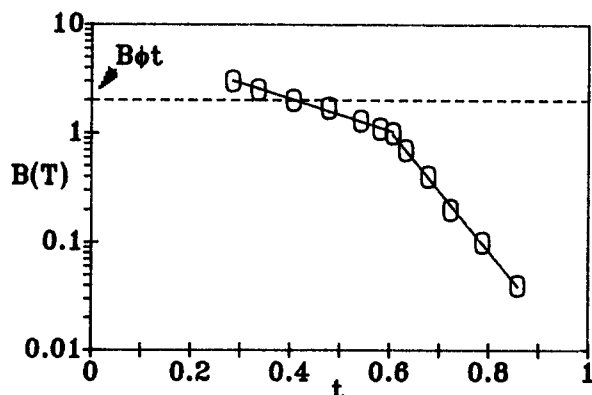


Figure 6 The irreversibility line of the Bi-2212 crystal irradiated by  $10^{11}$  Pb/cm<sup>2</sup> ( $B_{\phi t} = 2$ T). The straight lines are fits exhibiting the exponential dependence of  $B_{irr}(t)$  within the intermediate and high temperatures ranges.

6. Discussion.

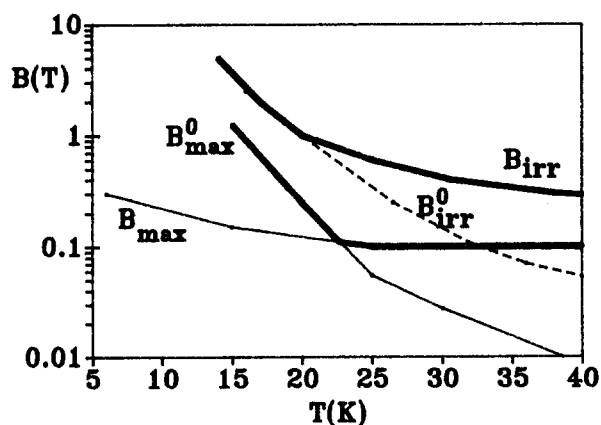


Figure 7  $B_{max}^0$ ,  $B_{max}$  and  $B_{irr}$  as functions of the temperature for a Bi-2212 crystal before and after irradiation at  $B_{\phi t} = 0.2$  Tesla. We have superimposed in dotted line the values of  $B_{irr}^0$  which corresponds to the irreversibility line before irradiation.

In figure 7 for  $B_{\phi t} = 0.2$  Tesla we have reported on the same figure the values of  $B_{irr}^0$  and  $B_{max}^0$  obtained before irradiation.  $B_{max}$  and  $B_{max}^0$  do not present the same temperature dependence:  $B_{max}$  which is related to the columnar defects varies more slowly with the temperature than  $B_{max}^0$  since the irradiation induced defects are more effective for vortex pinning at high temperatures than the preexisting defects. One can observe a crossing between  $B_{max}$  and  $B_{max}^0$  at about 23K.  $B_{irr}$  presents the temperature dependence of  $B_{max}^0$  at low temperature and the temperature dependence of  $B_{max}$  at high temperature. Between 20K and 30K, there is a cross-over between the two regimes.

As stated here above, there is a giant effect of the pre-existing defects at low temperature. In order to analyse this effect more precisely, we have reported in figure 8 the critical current density as a function of  $B - B_{\phi t}$  for different values of  $B_{\phi t}$ .  $B - B_{\phi t}$  is proportional to the difference between the number of vortices and the number of tracks. At 6K and 15K, all the curves merge at  $B > B_{\phi t}$  the value of the critical current before irradiation. In a recent experiment, Gerhauser et al. (40) have also observed that the critical current density at 10K at  $B = B_{\phi t}$  is independent of  $B_{\phi t}$  after irradiation of Bi-2212 crystals by 0.5 GeV I ions which create the same type of columnar defects. Our measurements above 15K show that this is not true at higher temperatures. Moreover, the independence of the critical current density is valid not only at  $B = B_{\phi t}$  but also for  $B > B_{\phi t}$ . In a simple model in which all the vortices are pinned in the tracks,  $B - B_{\phi t}$  measures the number of vortices which are not pinned in the tracks: the "track-unpinned" vortex. The conclusion of our observation is that the critical current density is driven by the pinning of the track-unpinned vortices on the defects which already exist in the crystal before irradiation.

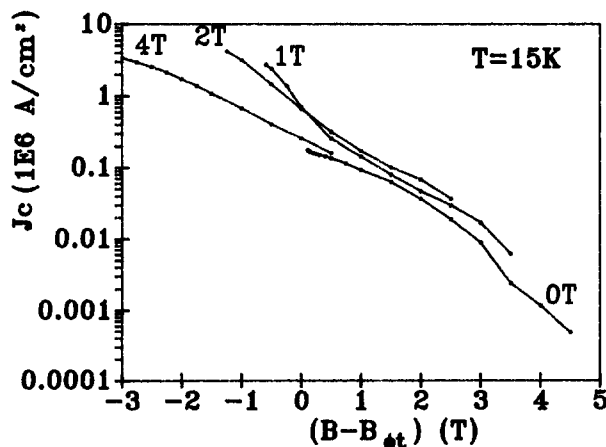


Figure 8 The critical current density  $J_c$  as a function of  $B - B_{\phi t}$  for different track densities at  $T = 15$ K

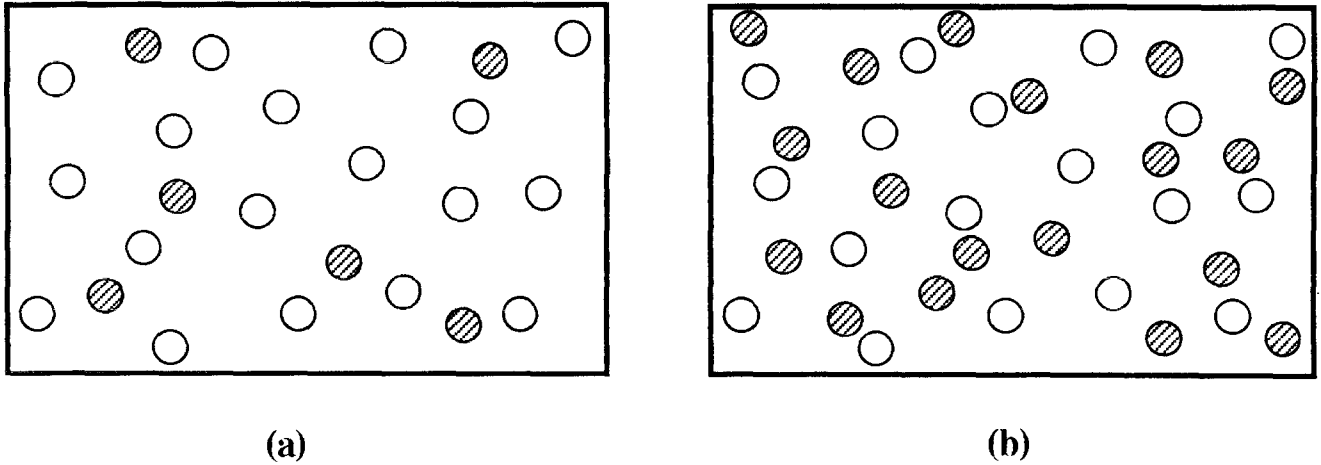


Figure 9 Schematic drawing of the track-pinned (black) and track-unpinned (white) vortices for a same number of track-unpinned vortices and a same critical current density:

- (a) for small values of  $B_{\phi_t}$  with  $B > B_{\phi_t}$   
 (b) for high values of  $B_{\phi_t}$  for  $B > B_{\phi_t}$ .

In figure 9, the situation of the vortex state for  $B > B_{\phi_t}$  has been schematically drawn, assuming a simple model in which all the tracks are occupied: for small values of  $B_{\phi_t}$ , the vortices flow around the tracks without interactions (figure 9a); as  $B_{\phi_t}$  increases, this remains true though each unpinned vortex is now surrounded by pinned vortices (figure 9b). This implies that the shear modulus  $C_{66}$  of the vortex lattice is small enough to avoid any elastic interaction between track-pinned and track-unpinned vortices. Such a model would explain the systematic shift of  $F_p$  observed for example on figure 2. Indeed if one assumes that  $j_c(B) = j_c^0(B - B_{\phi_t})$ , one can write that:

$$F_p(B) = F_p^0(B - B_{\phi_t}) B / (B - B_{\phi_t}) \quad (2)$$

which involves a shift of the maximum and an increase of  $F_p^{\max}$  indeed in agreement with the results reported on figure 2.

## 7. Conclusion

We have presented an investigation of 6 GeV Pb ion irradiation effects on the volume pinning forces, on the irreversibility line and on the critical current density in Bi-2212 crystals. The main concluding remarks can be summarized as follows:

i) When all the Pb-ion induced tracks are occupied, the critical current density is driven by the pinning of the track-unpinned vortices on the defects which already exist in the crystal before irradiation. This implies that the

shear modulus  $C_{66}$  of the vortex lattice is rather small. This rules out the melting of the vortex lattice as an explanation of the irreversibility line.

The magnetic field  $B_{\max}$  due to the Pb ion tracks is close to the dose equivalent field  $B_{\phi_t} = n_{\phi_t} \phi_0$ , suggesting a "matching" effect. It results that the order of magnitude of  $B_{\max}$  is controlled by the defect density  $n_{\phi_t}$ . The exact value of  $B_{\max}$  should be determined by a competition between pinning and vortex repulsion.

ii) The location of the IL is strongly dependent upon the density of the induced columnar defects but three main ranges of temperature must be distinguished:

(1) at low temperatures (around  $T < 15K$ ), the irreversibility line does not change with respect to that obtained before irradiation. In this range, the IL is likely only driven by the background defects present in the sample prior to irradiation.

(2) in a wide intermediate range of temperature, the irreversibility line is dominated by the pinning by the induced columnar defects. We can observe, in this intermediate range of temperature, that the IL shift induced by columnar defects is stronger than those associated with less extended defects (caused by neutrons (6,29) or protons (41) for instance).

(3) at high temperatures, a crossover in the FLL behaviour has been observed. It has been related to a 3D to 2D transition already reported in the Bi-2212 superconductor (32). Close to  $T_c$ , the 2D behaviour ( $L_c$  inferior to the distance between the  $CuO_2$  sheets) does not allow the current transport without dissipation. Under this transition line, in the so-called "3D phase", efficient vortex pinning is possible.

## Acknowledgements

The authors would like to thank S. Durcok (CSAV Prague) for providing Bi-2212 single crystals, J.P. Chaminade and J.C. Frison (LCS Bordeaux) for Tl-based single crystals. They are also indebted to S. Bouffard for his help during the irradiation experiments performed at the national laboratory GANIL (Caen).

## References

- 1 K.A. Müller, M. Takashige and J. G. Bednorz, *Phys. Rev. Lett.* 58 (1987) 1143.
- 2 R.B. van Dover, E.M. Gyorgy, F.F. Schneemeyer, J.W. Mitchell, K.V. Rao, R. Puzniak and J.V. Waszczak, *Nature* 342 (1989) 55.
- 3 F.M. Sauerzopf, H.P. Wiesinger, W. Kritscha, H.W. Weber, G.W. Crabtree and J.Z. Liu, *Phys. Rev.* B43 (1991) 3091.
- 4 J.O. Willis, D.W. Cooke, R.D. Brown, J.R. Cost, J.F. Smith, R.M. Aikin and M. Macz, *Appl. Phys. Lett.* 53 (1988) 417.
- 5 D. Bourgault, S. Bouffard, M. Toulemonde, D. Groult, J. Provost, F. Studer, N. Nguyen and B. Raveau, *Phys. Rev.* B39 (1989) 6549.
- 6 L. Civale, A.D. Marwick, T.K. Worthington, M.A. Kirk, J.R. Thompson, L. Krusin-Elbaum, Y. Sun, J.R. Clem and F. Holtzberg, *Phys. Rev. Lett.* 67 (1991) 648.
- 7 Th. Schuster, M.R. Koblischka, H. Kuhn, H. Kronmüller, M. Leghissa, W. Gerhäuser, G. Saeman-Ischenko, H.W. Neumüller, S.Klaumünzer, *Phys. Rev. B* 46 (1992) 8496.
- 8 V. Hardy, J. Provost, D. Groult, M. Hervieu, B. Raveau, S. Durcok, E. Pollert, J. C. Frison, J. P. Chaminade and M. Pouchard, *Physica C* 191, 85 (1992).
- 9 Y. Yeshurun and A.P. Malozemoff, *Phys. Rev. Lett.* 60, 2202 (1988).
- 10 P. H. Kes, J. Aarts, J. van den Berg, C. J. van der Beek and J. A. Mydosh, *Supercond. Sci. Technol.* 1, 242 (1989).
- 11 A. Houghton, R. A. Pelcovits and A. Sudbo, *Phys. Rev. B* 40, 6763 (1989).
- 12 M. P. A. Fisher, *Phys. Lett.* 62, 1415 (1989).
- 13 D. R. Nelson, *Physica C* 162-164, 1156 (1989).
- 14 W. Kritscha, F. M. Sauerzopf, H. W. Weber, G. W. Crabtree, Y. C. Chang and P. Z. Jiang, *Europhysics Lett.* 12, 179 (1990).
- 15 L. Civale, A. D. Marwick, M. W. Mc Elfresh, T. K. Worthington, A. P. Malozemoff, F. H. Holtzberg, J. R. Thompson and M. A. Kirk, *Phys. Rev. Lett.* 65, 1164 (1990).
- 16 M. Konczykowski, F. Rullier-Albenque, E. R. Yacoby, S. Shaulov, Y. Yeshurun and P. Lejay, *Phys. Rev. B* 44, 7167 (1991).11)
- 17 W. Gerhäuser, H. W. Neumüller, W. Schmidt, G. Ries, G. Saemann-Ischenko, H. Gerstenberg and F. M. Sauerzopf, M2S-HTSC, Kanazawa (1991).
- 18 V. Hardy, J. Provost, D. Groult, B. Raveau, L. R. Tessler, J. C. Frison, J. P. Chaminade and S. Bouffard, *Mat. Sci. Eng. B* 13, 279 (1992).
- 19 D. Bourgault, M. Hervieu, S. Bouffard, D. Groult and B. Raveau, *Nucl. Instr. and Meth. B* 42, 61 (1989).
- 20 B. Roas, B. Hensel, S. Henke, S. Klaumünzer, B. Kabius, W. Watanabe, G. Saeman-Ischenko, L. Schultz and K. Urban, *Europhys. Lett.*, 11 (1990) 669.
- 21 E.J. Kramer, *J. Appl. Phys.* 44 (1973) 1360.
- 22 A.M. Campbell, J.E. Evetts, *Adv. Phys.* 21 (1972) 199.
- 23 W.A. Fietz and W.W. Weeb *Physical Review*, Vol. 178 n°2 (1969) 657.
- 24 L. Civale, M.W. Elfresh, A.D. Marwick, F. Holtzberg, C. Feild, J. R. Thompson, D.K. Christen, *Phys. Rev. B* 43 (1991) 13732.
- 25 V.M. Pan, S.V. Gaponov, G.G. Kaminsky, D.V. Kuzin, V.I. Matsui, V.G. Prokhorov, M.D. Strikovskiy and C.G. Tretiaichenko, *Cryogenics* 29 (1989) 392.
- 26 T. Nojima, T. Fujita, *Physica C* 178 (1991) 140.
- 27 L. W. Song, M. Yang, E. Chen, Y. H. Kao, *Phys. Rev. B* 45 (1992) 3083.
- 28 L. W. Lombardo, D. B. Mitzi, A. Kapitulnik and A. Leone, *Phys. Rev. B* 46 (9), 5615 (1992).
- 29 H.W. Weber, *Supercond. Sci. Technol.* 5 (1992) 519.
- 30 H. Raffy, E. Guyon, J.C. Renard, *Solid St. Com.* 14 (1974) 427.
- 31 H. Raffy, E. Guyon, J.C. Renard, *Solid St. Com.* 14 (1974) 431.
- 32 H. Raffy, S. Labdi, O. Laborde and P. Monceau, *Physica C* 184 (1991) 159.
- 33 T. T. M. Palstra, B. Batlogg, L. F. Schneemeyer, R. B. van Dover and J. V. Waszczak, *Phys. Rev. B* 38 (1988) 5102.
- 34 G. Deutscher and A. Kapitulnik, *Physica A* 168 (1990) 338.
- 35 P. de Rango, B. Giordanengo, R. Tournier, A. Sulpice, J. Chaussy, G. Deutscher, J.L. Genicon, P. Lejay, R. Retoux and B. Raveau, *J. Phys. (Paris)* 50 (1989) 2857.
- 36 W. E. Lawrence and S. Doniach, in: *Low Temperature. Physics LT12*, ed. E. Kanda (Keigaku, Tokyo, 1971), p 361.
- 37 V. M. Vinokur, P. H. Kes and K. V. Koshelev, *Physica C* 168 (1990) 29.
- 38 M. V. Feigel'man, V. B. Geshkenbein and A. I. Larkin, *Physica C* 167 (1990) 117.
- 39 L. Krusin-Elbaum, L. Civale, F. Holtzberg, A.P. Malozemoff and C. Feild, *Phys. Rev. Lett.* 67 (1991) 3156.
- 40 W. Gerhäuser, G. Ries, H.W. Neumüller, W. Schmidt, D. Eibl, G. Saeman-Ischenko and S. Klaumünzer, *Phys. Rev. Lett.* 68 (1992) 879.
- 41 L. W. Lombardo, D. B. Mitzi, A. Kapitulnik and A. Leone, *Phys. Rev. B* 46 (1992) 5615.